



ELSEVIER

Journal of Magnetism and Magnetic Materials 238 (2002) 38–46



www.elsevier.com/locate/jmmm

Relation between grain alignment and magnetic properties of Pr–Fe–B sintered magnets

R.N. Faria*, A.R.M. Castro, N.B. Lima

Instituto de Pesquisas Energéticas e Nucleares IPEN-CNEN, CEP 05422-970, Sao Paulo, Brazil

Received 10 May 2001; received in revised form 6 September 2001

Abstract

This paper presents the results of investigations carried out to correlate magnetic properties and grain alignment in some as-sintered and heat treated Pr–Fe–B magnets. Sintered magnets based on the composition $\text{Pr}_{16}\text{Fe}_{76}\text{B}_8$ were prepared using the hydrogen deprecation process. Magnetic behaviour (B_r and iH_c) was studied as a function of degree of grain alignment ($\langle \cos \theta \rangle$). The volume fraction (f) of the matrix phase Φ ($\text{Pr}_2\text{Fe}_{14}\text{B}$ grains) in the permanent magnets was also estimated and correlated with intrinsic coercivity. © 2002 Elsevier Science B.V. All rights reserved.

Keywords: Magnets; Texture; PrFeB-alloys

1. Introduction

It is well known that to be able to achieve full performance for any hard magnetic material, it is essential to produce the material in a magnetically anisotropic form. Even though isotropic magnets are capable of large coercivities, their remanence is restricted to only half of the saturation magnetization at high fields. The process of introducing magnetic anisotropy consists of orienting the granular material with the easy magnetic axis of the particles oriented parallel to one another. In standard powder metallurgy, this is carried out magnetically with a pulsed or static field, prior to the pressing and sintering stages. Each powder particle must be a single crystal, for it to orient. Hence, milling of the starting material is carried

out to produce a narrow size distribution of single crystal particles [1]. Ultimately, this stage controls the degree of grain alignment of a permanent sintered magnet (provided the particle orientation field is strong enough).

The preparation of sintered magnets from rare earth (RE) based powders becomes difficult when powders with fine particle sizes are to be sintered. A dramatic decrease in remanence and intrinsic coercivity of sintered magnets has been reported when the particle size decreases below a critical value [2]. The remanence behaviour was similar to the intrinsic coercivity. This was attributed to oxidation of the fine powders. It has also been reported that overmilling reduces the intrinsic coercivity by damaging the particle surface [1].

Studies on sintered RE iron boron magnets have shown that improvements in grain alignment lead to reduction of coercivity, due to increase in internal demagnetizing fields [3]. On the other

*Corresponding author.

E-mail address: rfaria@net.ipen.br (R.N. Faria).

hand, it has also been reported [4] that the commonly observed decrease of coercivity with improved grain alignment is not an inevitable correlation in RE–Fe–B permanent magnets. In materials with high coercivity, improved grain alignment should also lead to increase in the coercive field. In Pr–Fe–B permanent magnets, the remanence increases with increase in milling time, and is accompanied by a decrease in coercivity [5]. Furthermore, this increase in remanence was attributed to increase in the degree of grain alignment in these magnets [6].

In this investigation, attempts have been made to correlate magnetic behaviour and the degree of crystal alignment of various Pr₁₆Fe₇₆B₈ sintered magnets. Although it is possible to vary the degree of alignment in sintered magnets, by changing the intensity of the orientation field, in this investigation the milling stage was used to change the degree of grain alignment in Pr–Fe–B sintered magnets. Attempts have also been made to correlate the magnetic behaviour of these Pr–Fe–B hydrogen decrepitation (HD) sintered magnets with the corresponding volume fraction of the Pr₂Fe₁₄B grains.

2. Experimental

The chemical analysis of the cast Pr₁₆Fe₇₆B₈ alloy, details about the preparation of the HD-sintered magnets, the post-sintering heat treatment and the magnetic measurements have been described in a previous paper [5]. The HD material was milled in a roller ball-mill. The oriented powder (in a pulsed field of 6 T) was pressed in an isostatic press. This method allowed fewer pressure-activated processes to take place, compared to uniaxial pressing in a die [7]. The degree of easy-axis alignment of the Pr₂Fe₁₄B matrix grains in these magnets was determined by X-ray pole figure analysis using the (004) reflection, which has also been described in detail elsewhere [6]. The saturation polarization of a Pr–Fe–B alloy was taken as the product of the volume fraction (f) of the matrix phase and the spontaneous polarization (I_s) of the Pr₂Fe₁₄B matrix phase (fI_s) [8]. The volume fraction ($0 \leq f \leq 1$) of the Pr₂Fe₁₄B

matrix phase was estimated from the expression [9]:

$$B_r = \langle \cos \theta \rangle f P I_s, \quad (1)$$

where B_r is the remanence of the Pr–Fe–B HD-sintered magnets. $\langle \cos \theta \rangle$ is the (average) degree of easy axis alignment of the Pr₂Fe₁₄B matrix phase grains; this is 0.5 for an isotropic magnet and increases to 1 for a perfectly aligned magnet. The value of I_s for the Pr₂Fe₁₄B matrix phase is 1.575 T at 293 K [10]. The packing factor ($P = \text{magnet density/theoretical density}$) for Pr₁₆Fe₇₆B₈ HD-sintered permanent magnets is ~ 0.98 [11] (calculated density: 7.513 g cm⁻³ [12]).

3. Results and discussion

The milling time, degree of alignment, density, volume fraction of the matrix phase and magnetic properties (before and after heat treatment at 1273 K for 86.4 ks) for the Pr₁₆Fe₇₆B₈ HD-sintered permanent magnets, are given in Table 1. The volume fraction of the matrix phase decreased with increase in milling time. The volume fraction of the matrix phase in Nd₁₆Fe₇₆B₈ alloy is reported to be 82% [13]. This is consistent with the range of values observed in the present investigation for Pr₁₆Fe₇₆B₈ HD-sintered magnets. It can be noted in Table 1 that the values of the degree of easy axis alignment increase with increase in the squareness factor ($SF = H_k/H_c$). Previous attempts [14] to correlate these two parameters for Sm–Co permanent magnets showed a wide scatter and no meaningful conclusions were drawn. The density (ρ) of the HD magnets was close to the calculated value and the packing factor, around 0.97–0.98.

The effects of milling time and heat treatment on the degree of alignment of the Pr₁₆Fe₇₆B₈ magnets are shown in Fig. 1. There is an increase in the degree of alignment with milling time and this is due to increase in the proportion of single crystal particles (grains) obtained by milling. The final degree of alignment of a magnet prepared with very small single crystal particles should be higher than that for a magnet produced with (relatively) large single crystal particles, due to the easier rotation of the former in the applied orientation field (smaller moment of inertia). The increase in

Table 1
Magnetic properties of $\text{Pr}_{16}\text{Fe}_{76}\text{B}_8$ HD sintered magnets

Milling time $X (10^3)$ (s)	Processing condition	$\langle \cos \theta \rangle$ (± 0.01)	SF (ratio) (± 0.02)	B_r (T) (± 0.02)	$\mu_{0i}H_c$ (T) (± 0.02)	$\mu_{0b}H_c$ (T) (± 0.02)	$(\text{BH})_{\text{max}}$ (kJ/m ³) (± 5)	ρ (gcm ⁻³) (± 0.02)	f (± 0.02)
64.8	As-sintered	0.80	0.77	1.09	1.49	1.02	234	7.37	0.88
	Heat treated	0.88	0.81	1.09	1.75	1.05	232	7.38	0.80
97.2	As-sintered	0.88	0.79	1.10	1.32	1.00	228	7.38	0.81
	Heat treated	0.92	0.89	1.12	1.67	1.09	245	7.39	0.79
129.6	As-sintered	0.92	0.75	1.11	1.43	1.01	229	7.35	0.78
	Heat treated	0.95	0.81	1.12	1.53	1.07	245	7.37	0.76
162.0	As-sintered	0.96	0.84	1.14	1.39	1.06	248	7.32	0.77
	Heat treated	0.97	0.93	1.15	1.49	1.11	255	7.30	0.77

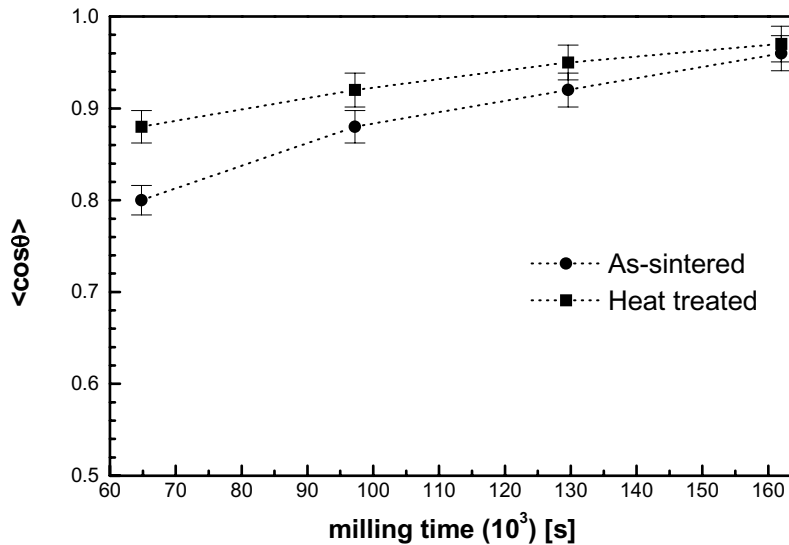


Fig. 1. Variation of degree of alignment of matrix phase grains of $\text{Pr}_{16}\text{Fe}_{76}\text{B}_8$ HD magnets with milling time.

$\langle \cos \theta \rangle$ with heat treatment was more pronounced for the magnets prepared using particles milled for a shorter time. Also, the magnet with the highest increase in degree of alignment with heat treatment (from 0.80 to 0.88; milling time: 64.8 ks) revealed the best intrinsic coercivity (1.75 T). This increase with heat treatment could be attributed to compositional homogenization taking place during this treatment, inducing the formation of some matrix phase in the alignment direction. No significant change in the degree of alignment with heat treatment was observed in the magnet prepared using powders milled for the

longest time (also with the highest degree of orientation, 0.97). It is well known that the powder metallurgy route tends to homogenize the material during the milling and sintering stages. Thus, the magnet-processing steps could cause progressive attenuation of the influence of ingot structure on the properties of the sintered magnet. Any homogenizing effects take place mostly during the milling stage and the influence of the initial as-cast structure of the alloy would be smaller after extended milling times.

Fig. 2 shows the variation of remanence with the degree of c -axis alignment for the $\text{Pr}_{16}\text{Fe}_{76}\text{B}_8$ HD

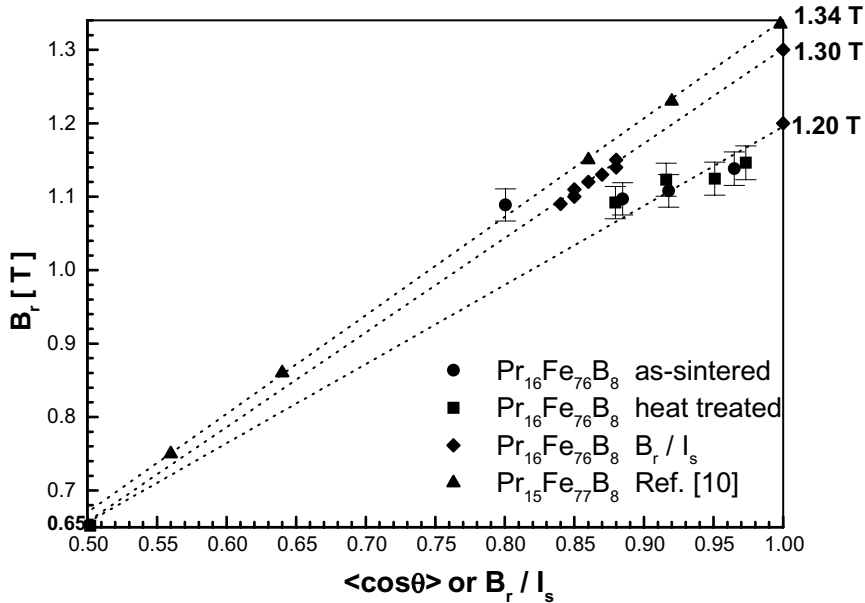


Fig. 2. Variation of remanence with degree of alignment of the matrix phase grains of $\text{Pr}_{16}\text{Fe}_{76}\text{B}_8$ HD magnets. $\text{Pr}_{15}\text{Fe}_{77}\text{B}_8$ magnet [10] data have been superimposed.

magnets, also in the as-sintered and heat treated conditions. Data from Ref. [10] for $\text{Pr}_{15}\text{Fe}_{77}\text{B}_8$ sintered permanent magnets (calculated using $I_s = 1.58$ T and $f = 0.85$) have also been plotted in Fig. 2, for comparison. The reported volume fraction of the matrix phase for a $\text{Nd}_{15}\text{Fe}_{77}\text{B}_8$ sintered magnet is 85% [15]. As expected, in both cases the remanence increases with increasing degree of alignment of the easy axis of the matrix $\text{Pr}_2\text{Fe}_{14}\text{B}$ grains. The origin of the graph shows the theoretical value for an isotropic $\text{Pr}_{16}\text{Fe}_{76}\text{B}_8$ magnet with a B_r of ~ 0.65 T ($0.5fI_s = 0.5 \times 0.82 \times 1.58$) and a $\langle \cos \theta \rangle$ of only 0.5. The dashed line joins this point to the present B_r values and indicates that the maximum remanence of the HD-sintered $\text{Pr}_{16}\text{Fe}_{76}\text{B}_8$ magnets would be around 1.2 T. A very similar value (1.19 T) was reported for sintered $\text{Pr}_{16}\text{Fe}_{76}\text{B}_8$ permanent magnets prepared by powder metallurgy [16]. According to Eq. (1), the theoretical remanence ($\langle \cos \theta \rangle = P = 1$, $f = 0.82$ and $I_s = 1.58$ T) for a magnet produced with this particular alloy is approximately 1.3 T (2×0.65 T). Using this value as the saturation

magnetization for this alloy, the ratio B_r/I_s was also plotted in Fig. 2 for comparison (this ratio is often used as the degree of alignment in magnets). In the case of the $\text{Pr}_{15}\text{Fe}_{77}\text{B}_8$ sintered magnets the isotropic value of remanence is 0.67 T ($0.5fI_s = 0.5 \times 0.85 \times 1.58$). A fully aligned sintered magnet would thus have a maximum remanence of 1.34 T (2×0.67). In this case there is an excellent fit between these two reference points and the data from Ref. [10] plotted in Fig. 2.

Fig. 3 shows the intrinsic coercivity and volume fraction of the matrix phase as a function of milling time, before and after annealing. Both parameters decrease with milling time. The decrease in intrinsic coercivity could be due to decrease in the volume fraction of the matrix phase with milling time. A similar decrease in iH_c has been observed in $\text{Nd}_{16}\text{Fe}_{76}\text{B}_8$ HD-sintered magnets [17] and the low values of intrinsic coercivity attributed to increased oxygen pickup during prolonged milling and to increased susceptibility to oxidation of the fine powders, as a result of the prolonged milling. The results obtained in

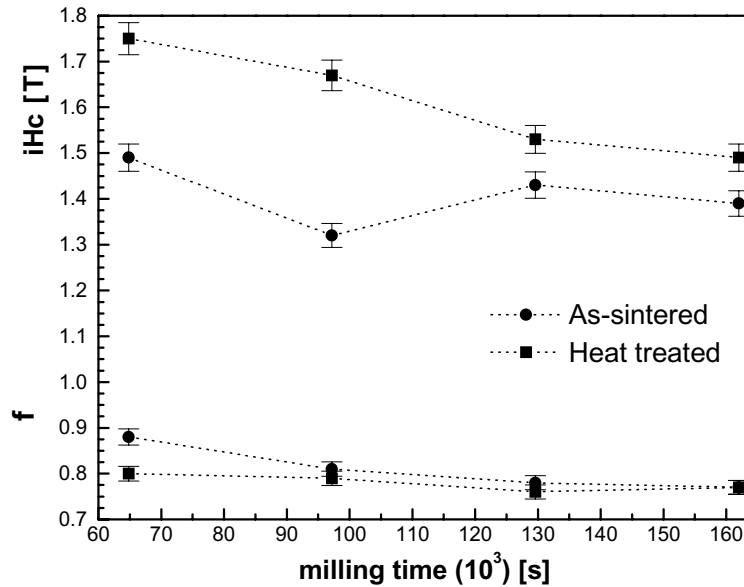


Fig. 3. Variation of coercivity of $\text{Pr}_{16}\text{Fe}_{76}\text{B}_8$ HD-sintered magnets and volume fraction of the matrix phase with milling time.

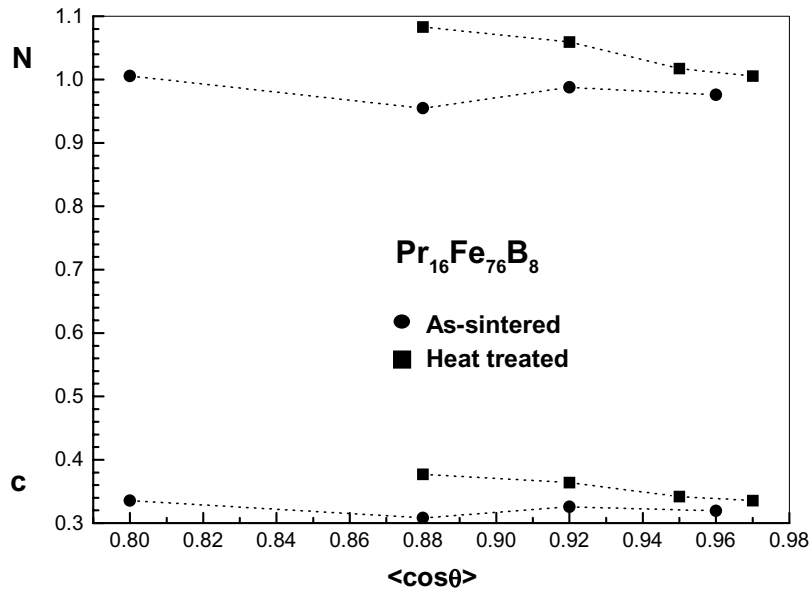


Fig. 4. Variation of microstructural parameters with degree of alignment of HD-sintered magnets.

this investigation indicate that oxidation by over-milling not only decreased the rare-earth-rich phase at the grain boundaries, but also some of the matrix phase (f decreased with milling time, as given in Table 1).

The increase in intrinsic coercivity (from 1.49 to 1.75 T) upon heat treatment was attributed previously [18] to improved isolation of the matrix phase by a nonmagnetic RE rich phase and smoothing of the grain boundaries in Pr-based

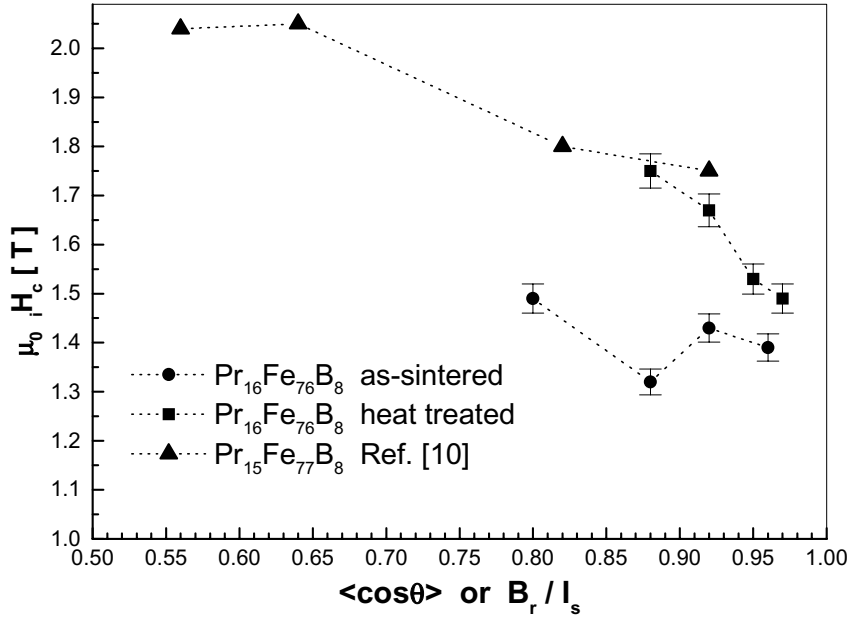


Fig. 5. Variation of coercivity of Pr₁₆Fe₇₆B₈ HD-sintered magnets with degree of alignment ($\langle \cos \theta \rangle$). Superimposed coercivities of sintered Pr₁₅Fe₇₇B₈ magnets were calculated using Eq. (2) (degree of alignment = B_r/I_s) and data from Ref. [10].

sintered magnets. The decrease in volume fraction of the matrix phase with heat treatment is consistent with either continued oxidation or loss of RE at high vacuum during heat treatment. Previous studies on Pr₁₅Fe₇₇B₈ magnets [10] have shown that intrinsic coercivity ($\mu_0 H_c$) in sintered magnets based on Pr₂Fe₁₄B can be described by

$$\mu_0 H_c = c\mu_0 H_A - NI_s, \quad (2)$$

$$N = 1.865c + 0.38, \quad (3)$$

where the magnetocrystalline anisotropy field ($\mu_0 H_A$) for the Pr₂Fe₁₄B matrix phase is 9.15 T (7.28 MA/m) and c and N are microstructural factors for the sintered magnet [10]. Assuming the absence of very large grains [10], these parameters were determined for the magnets using Eqs. (2) and (3) ($c = 0.16\mu_0 H_c + 0.097$). The values of intrinsic coercivity are given in Table 1. Fig. 4 shows the variation of c and N with the degree of alignment for the Pr₁₆Fe₇₆B₈ HD magnets. Both these parameters increase with heat treatment as also does the coercivity. According to Hiroswa

and Tsubokawa [10] the post-sintering heat treatment makes N smaller than for the as-sintered state and c remains unaltered. The post-sintering heat treatment of the HD magnets was carried out at a considerably higher temperature (for longer times). This treatment could affect these parameters differently, but not the coercivity behaviour. Fig. 5 shows the variation of intrinsic coercivity of the Pr₁₆Fe₇₆B₈ sintered and heat-treated magnets with degree of easy axis alignment, obtained using X-ray diffraction. The intrinsic coercivities of Pr₁₅Fe₇₇B₈ sintered magnets [10] calculated using Eq. (2) were also plotted as a function of the degree of alignment (B_r/I_s), for comparison. In both cases, coercivity decreased as the degree of alignment improved. The degree of alignment of the c -axis affected both c and N parameters [10]. Improved alignment yielded a smaller intrinsic coercivity, through the decrease in c , which overrode the effect of the reduction in N . Microstructural investigations and energy dispersive X-ray analysis are underway in an attempt to correlate the magnetic behaviour outlined in this paper, with microstructure.

Table 2

Degree of alignment and magnetic properties of $\text{Pr}_{16}\text{Fe}_{76}\text{B}_8$ sintered magnets produced from hydride powders and from partially as well as totally desorbed hydride powders (milling time: 64.8 ks)

Powder condition before milling	Processing condition	$\langle \cos \theta \rangle$ (± 0.01)	SF (ratio) (± 0.02)	B_r (T) (± 0.02)	$\mu_0 i H_c$ (T) (± 0.02)	$\mu_0 b H_c$ (T) (± 0.02)	$(\text{BH})_{\text{max}}$ (kJ/m ³) (± 5)
Fully hydrogenated	As-sintered	0.80	0.77	1.09	1.49	1.02	234
	Heat treated	0.88	0.81	1.09	1.75	1.05	232
Partially desorbed	As-sintered	0.96	0.66	1.13	1.45	1.00	247
	Heat treated	0.97	0.93	1.18	1.52	1.16	280
Totally desorbed	As-sintered	0.96	0.73	1.20	0.99	0.84	253
	Heat treated	0.97	0.79	1.22	1.06	0.89	286

The degree of alignment and magnetic properties of the standard HD-sintered $\text{Pr}_{16}\text{Fe}_{76}\text{B}_8$ magnets and sintered magnets in which hydrogen had been desorbed (partially or totally) from the powder [5] prior to the milling step are given in Table 2. Complete desorption of the HD material prior to magnet processing increased the remanence and decreased the intrinsic coercivity of the sintered magnets, compared to the corresponding properties of the standard HD magnets subjected to the same milling and heat treatments. The effect of partial desorption of the HD alloy prior to magnet processing also increased the remanence and decreased the intrinsic coercivity, but to a lesser extent than in the previous case. In both cases, the degree of alignment also improved substantially as a result of the desorption procedure. The magnetic behaviour of these magnets can be attributed to the effects of hydrogen on the magnetic properties of the powder. The differences in the degree of alignment of the milled powders can be partially attributed to reduced anisotropy of the $\text{Pr}_2\text{Fe}_{14}\text{B}$ phase in the HD powder. Further misalignment of the c -axis in HD-sintered magnets can occur with reduction in remanence, due to hydrogen induced partial spin reorientation [19]. Shape anisotropy and the presence of multi-grain particles can also reduce the degree of alignment [20]. Although the degree of alignment in the magnet produced from fully degassed powder (0.97) is not higher than that found in the $\text{Pr}_{16}\text{Fe}_{76}\text{B}_8$ HD-sintered magnet prepared using powders milled for longer times (162 ks), the remanence is slightly higher. The milling step

could also be affected by the degassing procedure and the higher remanence (1.22 T) of the magnet made from fully degassed powder, due in part to higher volume fraction of well-aligned single crystal ϕ phase grains in the magnet. The very low intrinsic coercivity of the magnet made from fully degassed powder can also be due to increase in oxygen content in the magnet, caused by the absence of hydrogen during the sintering of this material [21]. It has been reported [22] that the fraction of the ideal [001] texture component in Nd–Fe–B and NdDy–FeCo–B magnets was enhanced by doping with oxygen, resulting in a measurable increase in remanence and loop squareness associated with a small decrease in coercivity in the Nd–Fe–B magnets and a substantial increase in the iH_c of the Dy, Co-containing magnets.

Fig. 6 shows the energy product versus remanence for the $\text{Pr}_{16}\text{Fe}_{76}\text{B}_8$ HD-sintered magnet. The theoretical upper limit for the energy product ($B_r^2/4\mu_0$) for the $\text{Pr}_{16}\text{Fe}_{76}\text{B}_8$ HD-sintered magnets and for $\text{Pr}_{15}\text{Fe}_{77}\text{B}_8$ sintered magnets [10] are also included in the graph for comparison (valid for magnets with $bH_c \geq 0.5B_r$). The $(\text{BH})_{\text{max}}$ obtained for the magnets studied here are slightly below the theoretical values and indicate that the processing of the HD magnets was close to optimum. Fig. 7 shows the energy product versus intrinsic coercivity of totally desorbed (TD), partially desorbed (PD) and HD-sintered $\text{Pr}_{16}\text{Fe}_{76}\text{B}_8$ magnets. Magnetic properties of various Pr–Fe–B-type magnets taken from the literature [23–26] were superimposed for comparison. A feature of these Pr-based magnets

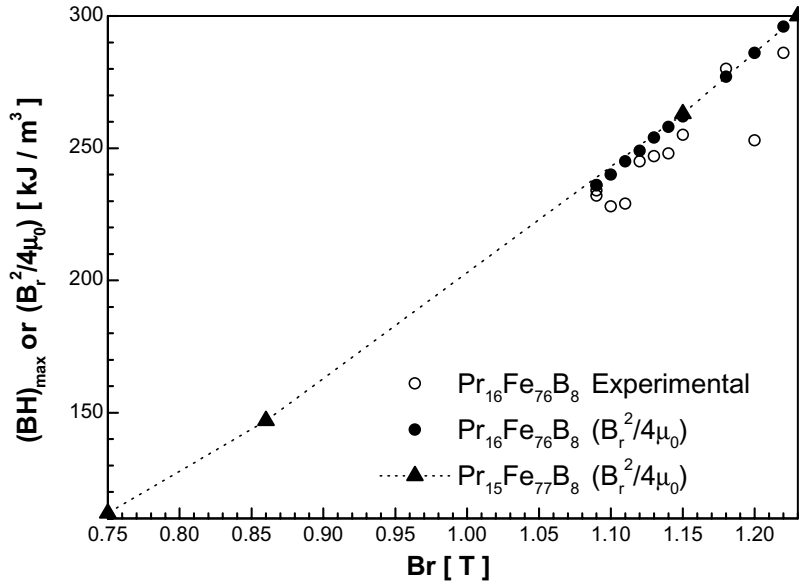


Fig. 6. Variation of energy product of $\text{Pr}_{16}\text{Fe}_{76}\text{B}_8$ HD-sintered magnets with remanence. $(B_r^2/4\mu_0)$ of sintered $\text{Pr}_{15}\text{Fe}_{77}\text{B}_8$ magnets were calculated using data from Ref. [10].

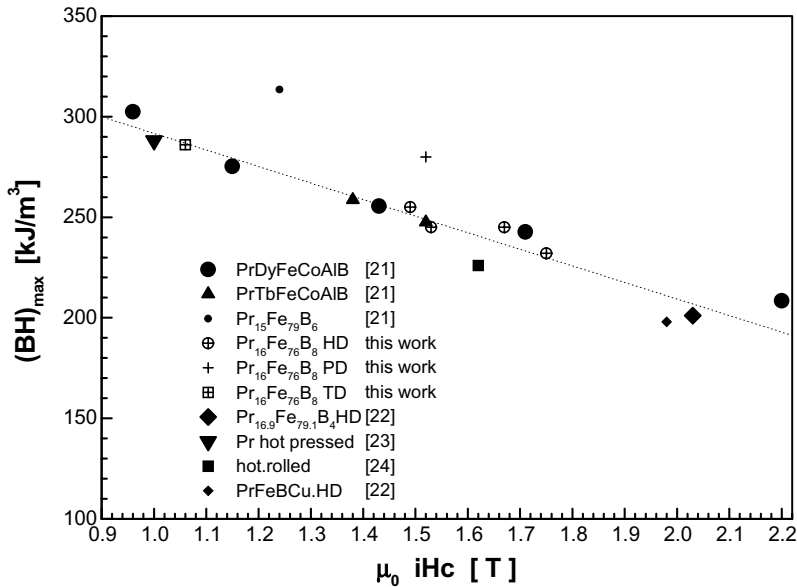


Fig. 7. Variation of energy product of $\text{Pr}_{16}\text{Fe}_{76}\text{B}_8$ sintered magnets with intrinsic coercivity. Superimposed $(\text{BH})_{\text{max}}$ of Pr–Fe–B-type sintered magnets were taken from Refs. [21–24].

is the inverse correlation of energy product (or remanence) and intrinsic coercivity. $\text{Pr}_{16}\text{Fe}_{76}\text{B}_8$ HD magnets in the as-sintered condition were not included, as coercivity had not fully developed.

Problems have been encountered in the production of large sintered blocks using the HD-process and these have been associated with the difficulty in removing hydrogen from within the block, prior

to the onset of sintering, and this results in the formation of cracks in the final product [21]. Avoidance of these cracks requires a carefully controlled degassing procedure and/or the use of partially degassed powder when pressing the green compacts [21]. As given in Table 2, magnets prepared with partially degassed material exhibit good overall magnetic properties.

4. Conclusions

The increase in remanence, with longer milling time, of the HD starting material is due to an increase in the degree of alignment of the sintered $\text{Pr}_{16}\text{Fe}_{76}\text{B}_8$ magnets. High degrees of orientation can be obtained with longer milling times, but better processing conditions or techniques need to be used to avoid degradation of intrinsic coercivity. The deterioration in coercivity with longer milling time has been attributed to decrease in volume fraction of the matrix phase. Post-sintering heat treatment is more effective with magnets that were prepared using shorter milling times.

Acknowledgements

Many thanks are due to FAPESP and IPEN-CNEN for supporting this investigation.

References

- [1] J. Ormerod, *J. Less-Common Met.* 111 (1985) 49.
- [2] C.N. Christodoulou, J. Schlup, G.C. Hadjipanayis, *J. Appl. Phys.* 61 (8) (1987) 3760.
- [3] G. Martinek, D.V. Kohler, H. Kronmuller, CEAM 2 Report, September 1991, unpublished work.
- [4] G. Martinek, H. Kronmuller, S. Hirosawa, *J. Magn. Magn. Mater.* 89 (1990) 369.
- [5] R.N. Faria, A.J. Williams, J.S. Abell, I.R. Harris, Proceedings of the 14th International Workshop on Rare-Earth Magnets and their Applications, São Paulo, 1996, p. 570.
- [6] A.R.M. Castro, K. Imakuma, M.M. Serna, N.B. Lima, Proceedings of the 15th International Workshop on Rare-Earth Magnets and their Applications, Dresden, 1998, p. 969.
- [7] H. Zwick, T. Schrefl, J. Fidler, *J. Appl. Phys.* 85 (8) (1999) 5672.
- [8] W. Fernengel, *J. Magn. Magn. Mater.* 83 (1990) 201.
- [9] C.W. Searle, V. Davis, R.D. Hutchens, *J. Appl. Phys.* 53 (3) (1982) 2395.
- [10] S. Hirosawa, Y. Tsubokawa, *J. Magn. Magn. Mater.* 84 (1990) 309.
- [11] R.N. Faria, H. Takiishi, L.F.C.P. Lima, I. Costa, *J. Magn. Magn. Mater.*, accepted.
- [12] T. Jinghua, H. Yiyang, L. Jingkui, *Scientia Sinica (Series A)* XXX (6) (1987) 607.
- [13] I.R. Harris, P.J. McGuinness, D.G.R. Jones, J.S. Abell, *Phys. Scripta* T19 (1987) 435.
- [14] D.L. Martin, H.F. Mildrum, S.R. Trout, Proceedings of the Eighth International Workshop on Rare-Earth Magnets and their Applications, Dayton, 1985, p. 269.
- [15] K.D. Durst, H. Kronmuller, *J. Magn. Magn. Mater.* 59 (1986) 86.
- [16] Z. Shouzeng, L. Lin, Z. Lidong, H. Qin, *J. Magn. Magn. Mater.* 54 (1986) 521.
- [17] P.J. McGuinness, Ph.D. Thesis, University of Birmingham, 1989, p. 160.
- [18] R.N. Faria, X.J. Yin, J.S. Abell, I.R. Harris, *J. Magn. Magn. Mater.* 129 (1994) 263.
- [19] D. Fruchart, L. Pontonnier, F. Vaillant, J. Bartolome, J.M. Fernandez, J.A. Puerltolas, C. Rillo, J.R. Regnard, A. Yaouanc, R. Fruchart, P. L'Heritier, *IEEE Trans. Magn. MAG* 24 (2) (1988) 1641.
- [20] S. Liu, *J. Appl. Phys.* 76 (10) (1994) 6757.
- [21] I.R. Harris, P.J. McGuinness, Proceedings of the 11th International Workshop on Rare-Earth Magnets and their Applications, Pittsburgh, 1990, p. 29.
- [22] A.S. Kim, F.E. Camp, H.H. Stadelmaier, *J. Appl. Phys.* 76 (10) (1994) 6265.
- [23] S.Y. Jiang, J.X. Yan, B.M. Ma, S.G. Sankar, W.E. Wallace, Paper No. 180202 at the Proceedings of the 10th International Workshop on Rare-Earth Magnets and Their Applications, Kyoto, Japan, 16–19 May, 1989, p. 457.
- [24] R.N. Faria, J.S. Abell, I.R. Harris, *J. Alloys Compounds* 177 (1991) 311.
- [25] T. Shimoda, K. Akioka, O. Kobayashi, T. Yamagami, T. Ohki, M. Miyagawa, T. Yuri, *IEEE Trans. Magn. MAG* 25 (5) (1989) 4099.
- [26] T. Shimoda, K. Akioka, O. Kobayashi, T. Yamagami, A. Arai, Paper No W1.2 at the Proceedings of the 11th International Workshop on Rare-Earth Magnets and Their Applications, Pittsburgh, PA, 21–24 October, 1990, p. 17.